

Development of an Ultrasonic Jig and Signal Analysis for Two-Phase Regime Detection

Che Zulnajmy Hazeeq Che Mohd Zawawi¹, Yasmin Abdul Wahab^{1*}, Mohd Mawardi Saari¹, Nurhafizah Abu Talip Yusof^{1,2}, Nurul Wahidah Arysad¹, Suzanna Ridzuan Aw³, Mohd Hafiz Fazalul Rahiman⁴, Jaysuman Puspanathan⁵, Ruzairi Abdul Rahim⁶, Sia Yee Yu⁷

¹Faculty of Electrical & Electronics Engineering Technology, Universiti Malaysia Pahang Al- Sultan Abdullah, 26600 Pekan, Pahang, Malaysia

²Centre for Research in Advanced Fluid & Processes (Fluid Centre), Universiti Malaysia Pahang Al-Sultan Abdullah, Lebuhraya Tun Razak, 26300 Gambang, Kuantan, Pahang, Malaysia

³Faculty of Electrical & Automation Engineering Technology, Terengganu Advance Technical Institute University College (TATiUC), Jalan Panchor, Telok Kalong, 24000 Kemaman, Terengganu, Malaysia

⁴Faculty of Electrical Engineering & Technology, Universiti Malaysia Perlis, 02600 Arau, Perlis, Malaysia

⁵School of Biomedical Engineering & Health Science, Faculty of Electrical Engineering, Universiti Teknologi Malaysia, 81310 UTM Skudai, Johor, Malaysia

⁶PROTOM-I Research Group, Faculty of Electrical Engineering, Universiti Teknologi Malaysia, 81310 UTM Skudai, Johor, Malaysia

⁷LOGO Solution Sdn. Bhd., suite 0525, Level 5, Wisma SP Setia, Jalan Indah 15, Bukit Indah, 79100 Iskandar Puteri Johor Malaysia

Corresponding author* email: yasmin@ump.edu.my

Available online 30 June 2025

ABSTRACT

The construction of an ultrasonic sensor jig and the ensuing signal analysis methods used for the identification of two-phase flow regimes are presented in this work. The sensor jig, which provides precise alignment of eight ultrasonic sensors (four transmitters and four receivers) around a testing vessel, was the main focus of the design of a portable ultrasonic tomography system. Accurate data collection depends on constant sensor alignment and non-invasive installation, which the sensor jig's Autodesk Fusion design makes possible. To handle the ultrasonic signals, electronic measurement circuits were developed, which included a signal generator and a signal conditioning unit. The system can distinguish between liquid and solid phases in a vertical position, according to experimental results. Variations based on sensor and phantom positions are shown by analyzing the first highest peak values of the received signals. The results demonstrated that the system successfully detected variations in the testing conditions, with output signal amplitudes ranging from 2 V to 15 V. This shows how sensitive the system is to changes in the two-phase medium. The sensor jig and signal analysis techniques that have been developed offer a basis for educational applications in real-time monitoring of multiphase flows and ultrasonic tomography.

Keywords: Ultrasonic Tomography, Sensor Jig, Liquid-Solid

1. Introduction

This Pipeline control and process monitoring in sectors such as chemicals and oil extraction depend heavily on the measurement of two-component flow, such as liquid or oil in pipes. The void fraction and flow regime can be determined with the aid of an understanding of flow distribution. For flow regimes that are always changing, real-time flow imaging is important. Controlling elements like flow rate and regime through accurate monitoring improves operational efficiency. An approach to fluid flow evaluation known as flow imaging is more thorough than the visual inspections or sampling methods used by industry in the past.

This project focuses on designing and developing a portable ultrasonic tomography system for educational purposes aimed at identifying two-phase regimes. The system will utilize advanced ultrasonic imaging techniques to accurately detect and visualize the distribution of different phases within a medium. Additionally, the project involves establishing circuit connections to measure the two-phase regimes specifically water-solid rod, mixtures inside a pipe, through an offline method. The sensor readings were analysed to evaluate the system's capability in detecting the liquid-solid regime.

2. Related Works on Ultrasonic Tomography

Advances in ultrasonic tomography have made it easier to observe and investigate two-phase flow regimes in both educational and industrial contexts. Among process tomography methods, ultrasonic tomography (UT) is unique since it is non-invasive, allows for real-time imaging, and can be adjusted to fit different vessel orientations. In order to get greater spatial resolution and more precise flow regime identification, current research has concentrated on enhancing sensor setups and signal processing techniques.

For example, the success of ultrasonic phased arrays in enabling omnidirectional, multi-point detection for high-resolution imaging and flow classification in vertical air-water flows was shown by Fang et al. [1]. Similar to this, Tan et al. [2] presented a modular ultrasonic phased array tomography system that is appropriate for complicated multiphase media in industrial applications due to its high spatial resolution and real-time monitoring. These research demonstrate how ultrasonic sensor configurations and signal analysis methods continue to advance, serving as the cornerstone for the creation of portable and instructive UT systems. Besides, Murakawa et al. [3] presented the development of a high-speed ultrasonic tomography system using a phased array sensor to visualize two-phase flow in a pipe, enabling real-time cross-sectional imaging. The system demonstrates improved imaging speed and accuracy, effectively distinguishing different flow regimes in dynamic two-phase flow conditions. Authors in Ref. [4] developed an innovative, non-invasive ultrasonic thermometry system for stainless-steel tanks, enabling precise temperature measurement without direct contact or intrusion. Their approach uses ultrasound transducers to achieve high accuracy and reliability, making it suitable for industrial environments where traditional sensors are limited. Lusheng Zhai et al. [5] designed a distributed ultrasonic sensor system to measure gas holdup in the slug region of horizontal oil-gas-water three-phase flow. Their results demonstrate that the system can effectively monitor gas distribution and holdup, providing valuable data for optimizing multiphase flow processes. Thus, this work builds on these advances by creating a special sensor jig and analyzing signals to better detect two-phase flow. This shows how important custom sensor setups and data analysis are for improving flow monitoring.

3. Related Principle for Ultrasonic Tomography

Acoustic impedance (Z) is a term used to describe the interaction of ultrasound with materials [6]. It is defined as the product of density (ρ) and the speed of sound (c) in the material, represented by the Equation (1):

$$Z = \rho c \quad (1)$$

Understanding acoustic impedances is crucial for several reasons as follows [7]:

- It determines the values of acoustic transmission and reflection at the boundary between two materials with different acoustic impedances.
- It is essential for designing ultrasonic transducers.
- It is important for assessing the absorption of sound in a medium.

The reflection coefficient (R) and transmission coefficient (T) equations are given as in Equation (2) and Equation (3) [8].

$$\text{Reflection coefficient, } R = \frac{P_r}{P_e} = \frac{Z_2 - Z_1}{Z_2 + Z_1} \quad (2)$$

$$\text{Transmission coefficient, } T = \frac{P_t}{P_e} = \frac{2Z_2}{Z_2 + Z_1} \quad (3)$$

In this case, Z represents acoustic impedance, P_e is an incident wave sound pressure, P_t is a transmitted wave sound pressure, and P_r is reflected wave sound pressure.

It is very important to know the ultrasonic propagation in all materials. Rather, the ultrasonic propagation between two materials can be understood through its reflection and transmission. The following describes the investigation of ultrasonic wave propagation for liquid medium (water) and gas medium (air), assuming that the ultrasonic energy losses between transducer coupling and PVC pipes are zero. For example, for ultrasonic wave propagation for water and air: Given that the acoustic impedance of water is $Z_1 = 1.5 \times 10^6 \text{ kg/m}^2$ and for air is $Z_2 = 0.4 \times 10^3 \text{ kg/m}^2$. By using Equation (2) and (3), the calculation of R and T can be expressed as:

$$R = \frac{P_r}{P_e} = \left[\frac{0.4 \times 10^3 - 1.5 \times 10^6}{0.4 \times 10^3 + 1.5 \times 10^6} \right] = -99.95\% \quad (4)$$

$$T = \frac{P_t}{P_e} = \left[\frac{2(0.4 \times 10^3)}{0.4 \times 10^3 + 1.5 \times 10^6} \right] = 0.0533\% \quad (5)$$

The negative sign Equation (4) indicates the reversal of the phase relative to the indicate wave. Based on Equation (5), it shows that the ultrasonic signal can transmit through water and air less than 1%. Hence, the the equations of T and R are important in predicting the percentage of signal transmission and receiving for each medium occurred.

4. Methodology

This project consists of a hardware system and a software system and designed like Figure 1 below. The hardware system includes both ultrasonic sensor and electronic measurement setups. The software system consists of Arduino Uno programming tools.

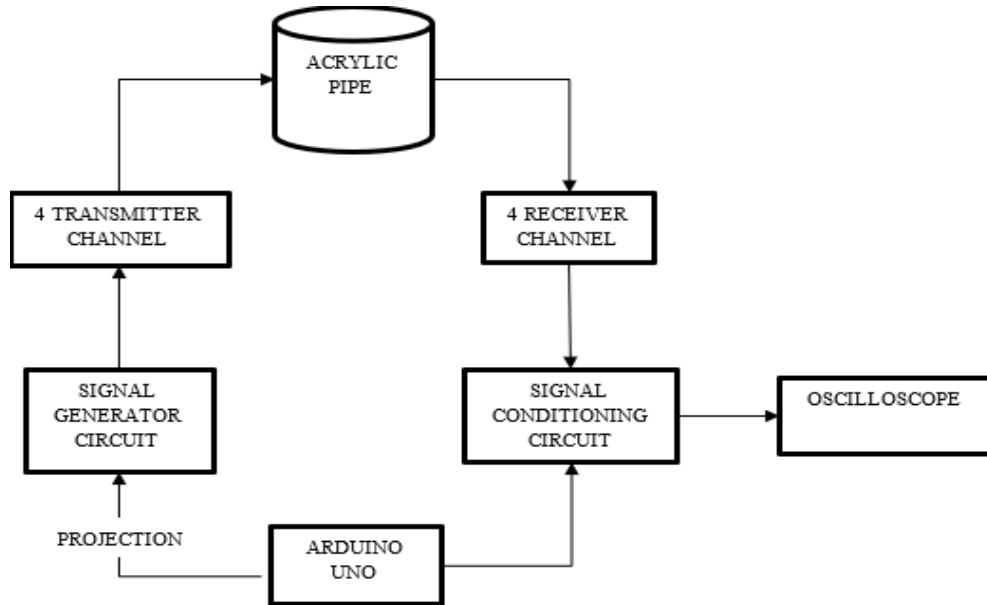


Figure 1. Block diagram of project

The hardware system consists of a signal generator, signal conditioning circuit, and Arduino Uno. The Arduino controls 40 kHz pulses to the signal generator, which supplies and amplifies the signal for the transmitter. The transmitter sends ultrasonic waves through the pipe, received by the receiver. The signals received are then amplified to a suitable voltage for oscilloscope observation.

Eight sensors (4 transmitters, 4 receivers) were non- invasively installed along the pipe wall using a transmission mode with a fan-shaped beam projection. The 4-transmitter, 4-receiver arrangement is shown in Figure 2.

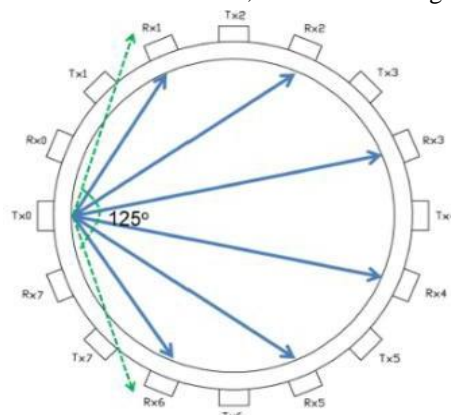


Figure 2. Sensor arrangement

The air ultrasonic ceramic transducer 400ET/R080 from Prowave Electronic Corporation was selected based on key criteria: beam angle, center frequency, driving voltage, and ease of mounting and coupling. Its closed-face design simplifies installation, while its sealed construction enhances durability against water, heat, and humidity. Operating at up to 15 Vrms with a 125-degree diverging angle, it meets project requirements effectively.

This project utilizes ultrasonic transducers in a non- invasive manner. Several methods were planned and evaluated before proceeding with the initial hardware implementation. Figure 3(a) illustrates the final design, which features an

acrylic pipe arranged in a vertical orientation, along with the sensor jig. The acrylic pipe used has a diameter of 60 mm, thickness of 3 mm and length of 170 mm. The sensor jig was designed using Autodesk Fusion software, as shown in Figure 3(b). The sensor jig also has a diameter of 60 mm, with eight strategically placed holes for ultrasonic sensors, each measuring 20 mm in diameter. The sensor jig can be easily removed and placed around the circumference of the outer tested pipe.

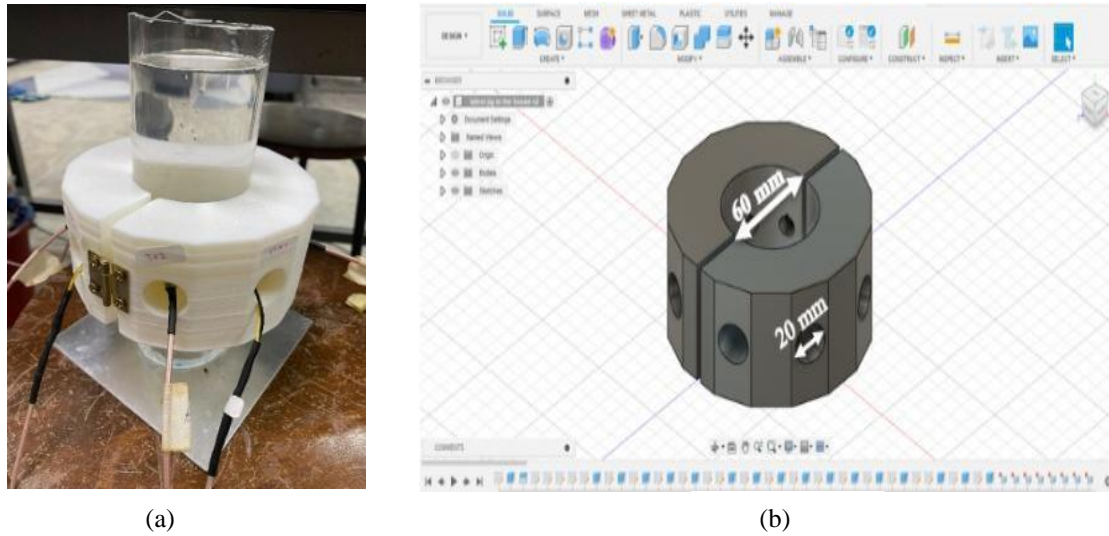


Figure 3. (a) Fabrication of sensor jig, (b) Sensor jig designed in Autodesk fusion software

The measurement technique consists of two circuits: the signal generator and signal conditioning circuits. The Arduino Uno was used as the microcontroller for this project. The two cycles of 40kHz square waveform with 100Hz delay for each channel was coded using the Arduino Uno. For the signal generator circuit, the excalibur low-noise, high-speed precision amplifiers, or the low-noise speed op- amp ic TLE2141CP from Texas Instruments was chosen to function as a comparator. Additionally, Figure 4(a) displays the schematic diagram of the signal generator circuit, while Figure 4(b) depicts the actual signal generator circuit in operation.

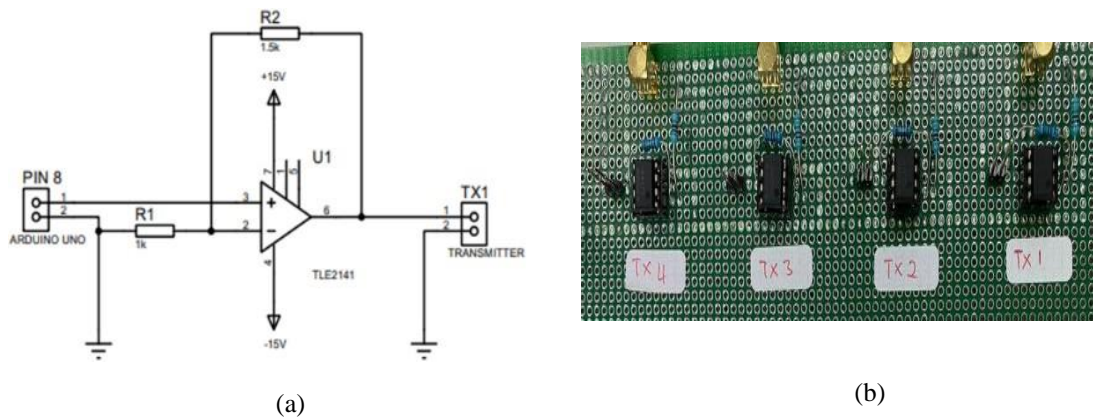


Figure 4. (a) Schematic diagram of signal generator circuit, (b) Real signal generator circuit

The non-inverting amplifier circuit was designed such that:

$$V_{out} = \left(1 + \frac{R_F}{R_1}\right) V_{in} = \left(1 + \frac{1.5k}{1k}\right) 5 = 12.5 V$$

The comparator generates a 12.5 Vp-p, 40 kHz tone burst with a 10 ms reverberation delay. Figure 5 shows the transmitted signal, where the output voltage gain is 13.8 Vpp instead of 12.5 Vpp due to initial piezoelectric vibration upon connection. This delay ensures reverberation dissipates before the next excitation, preventing overlapping echoes at the receiver.

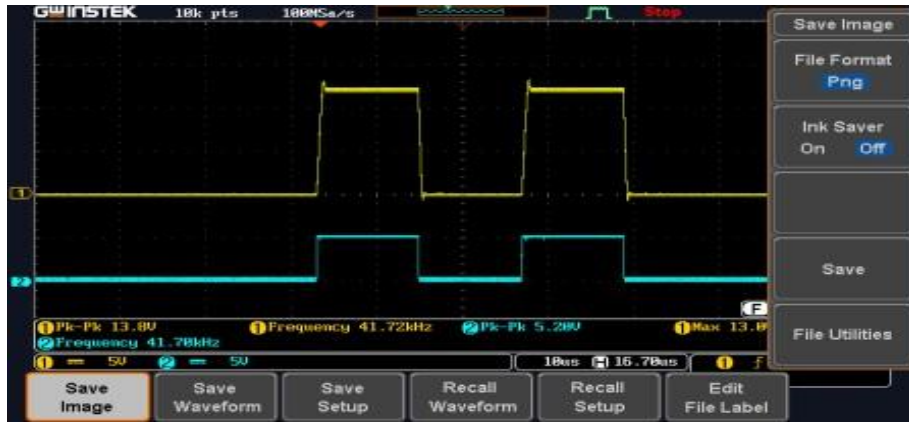


Figure 5. Output signal from Arduino Uno (blue line) and signal generator circuit (yellow line)

Then, the signal conditioning circuit includes the amplifier section, as shown in Figure 6. The LT1361 high-speed op-amp was selected for its 50 MHz bandwidth, 1000 V/μs slew rate, and stability. Its design enables fast, low-noise signal processing without extra components. With internal gain settings and a wide supply range ($\pm 2.5V$ to $\pm 15V$), it suits active filters and high-frequency amplification. Its low distortion ensures precise performance. The amplifier section maintains proper voltage gain, preventing signal clipping. Figure 7 displays the conditioned output signal (blue) and the first highest peak voltage measurement. Each receiver channel for each transmitted signal were then recorded for analysis purposes.

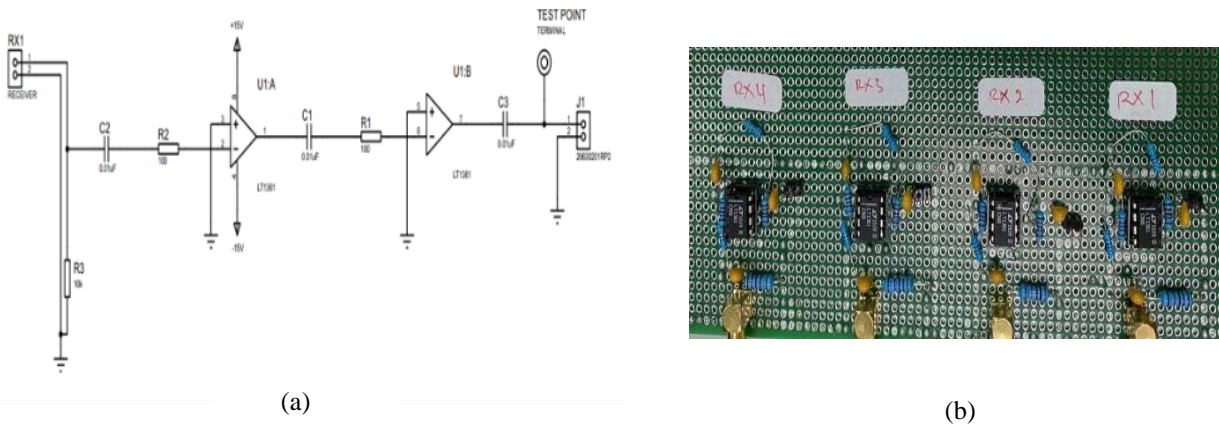


Figure 6. (a) Schematic diagram of signal conditioning circuit, (b) Real signal conditioning circuit

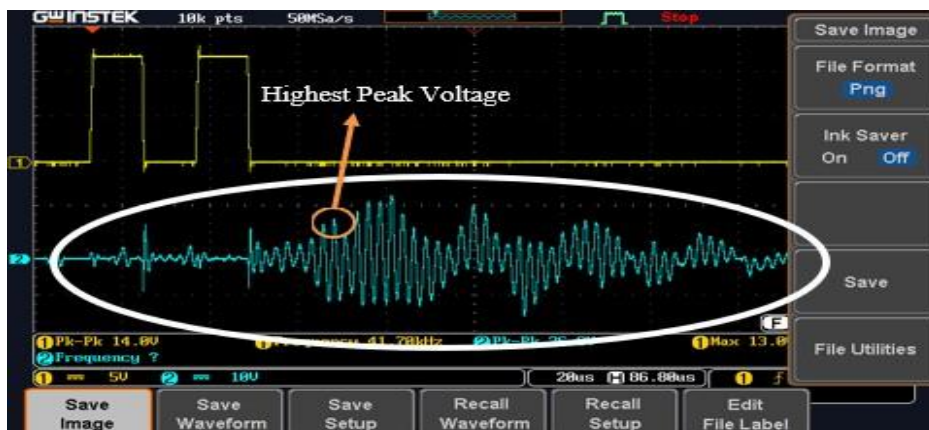
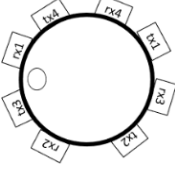
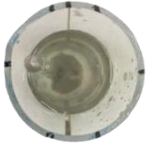
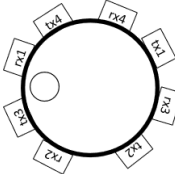
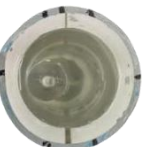
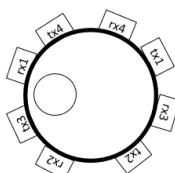
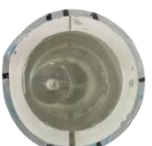
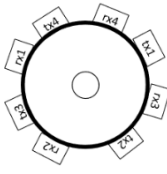

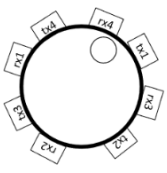

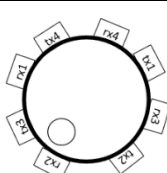



Figure 7. Output for signal conditioning circuit in blue line

5. Results and Discussion

Several tests were conducted to evaluate the sensor reading performance. These tests involved varying both the size and location of a hollow acrylic pipe used as a phantom. Phantoms with diameters of 10mm, 15mm, and 20mm at left position were tested, and three different locations (center, top right, and bottom left) with 15mm in diameter of phantom were also examined. Table 1 shows the size and location of the tested phantom.

Table 1. Size and location of tested phantom

Size and Location		Geometry	Real picture from top
Different sizes at left position	10mm		
	15mm		
	20mm		
Different location	Center		
	Top Right		
	Bottom Left		

The graph of the first highest peak value of the received signal measured when channel 1 as transmitter (Tx1) has been plotted and presented in Figure 8. It can be observed that the voltage depends on the sensor and phantom positions. At Tx1-Rx1 and Tx1-Rx2, larger phantom diameters reduce the voltage compared to full water. However, at Tx1-Rx3 and Tx1-Rx4, the voltage remains high since the receivers are next to Tx1. This confirms that closer transmitter-receiver placement results in higher voltage when unobstructed.

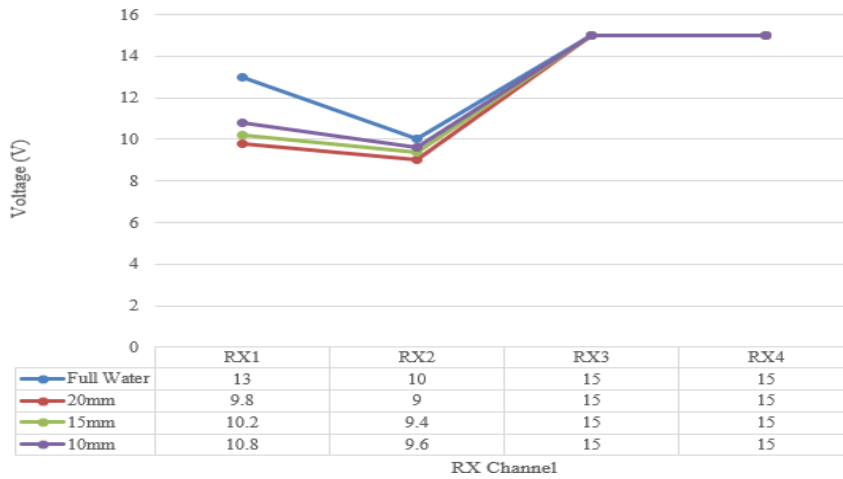


Figure 8. Line graph of first highest peak value of received signal measured for different diameters of phantom at the same position

The graph of the first highest peak value of the received signal measured has been plotted and is presented in Figure 9. The received voltage varies based on sensor and phantom positions. For Tx1-Rx1, Rx2, Rx3, and Rx4, the 15 mm phantom at the center and top right results in lower peak voltages than full water, except for Tx1-Rx3 and Tx1-Rx4 at the bottom left. This suggests signal obstruction reduces received voltage. However, for Tx1-Rx3 and Tx1-Rx4, the voltage remains high due to their proximity to Tx1. The data confirms that closer transmitter-receiver pairs yield higher voltages when unobstructed.

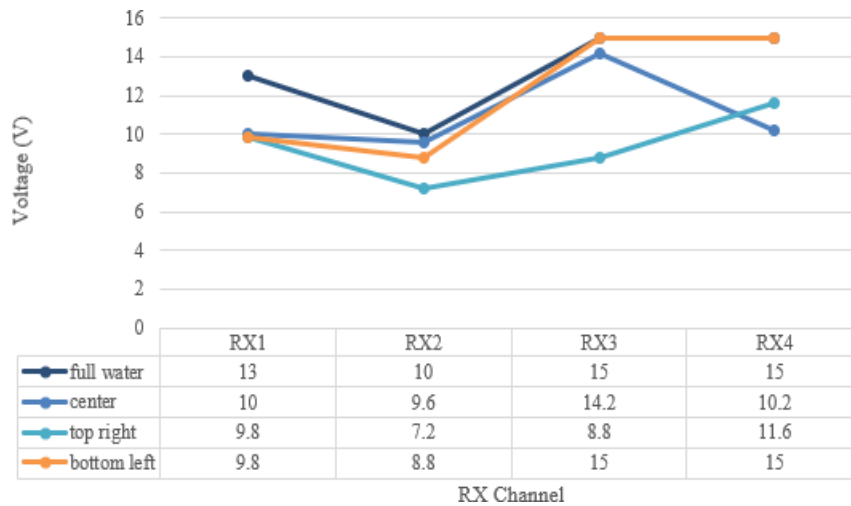


Figure 9. Line graph of first highest peak value of received signal measured for same diameters of phantom at different positions

6. Conclusion

In this work, a portable ultrasonic tomography system featuring a custom-designed sensor jig was successfully developed and tested for two-phase flow regime detection. The sensor jig enabled precise and repeatable alignment of eight ultrasonic sensors, ensuring reliable data collection and non-invasive installation. Experimental results demonstrated that the system could effectively distinguish between liquid and solid phases, with sensor readings sensitive to both the size and position of the inserted phantom. The analysis of signal amplitudes confirmed the system’s capability to detect variations in the two-phase medium, validating the effectiveness of the jig design and signal processing approach. Overall, the developed system provides a practical foundation for educational applications and further research in real-time multiphase flow monitoring using ultrasonic tomography.

Acknowledgment

The authors would like to thank the Universiti Malaysia Pahang Al-Sultan Abdullah for providing financial support and laboratory facilities.

References

- [1] L. Fang *et al.*, "Identification of two-phase flow regime using ultrasonic phased array," *Flow Meas. Instrum.*, vol. 72, no. September 2019, p. 101726, 2020, doi: 10.1016/j.flowmeasinst.2020.101726.
- [2] C. Tan, Z. Zhang, H. Liu, R. Fu, G. Yang, and F. Dong, "Ultrasonic phased array process tomography system for multiphase medium imaging," *IEEE Trans. Instrum. Meas.*, vol. 72, no. 2, p. 1, 2023, doi: 10.1109/TIM.2023.3271756.
- [3] H. Murakawa, T. Shimizu, and S. Eckert, "Development of a high-speed ultrasonic tomography system for measurements of rising bubbles in a horizontal cross-section," *Meas. J. Int. Meas. Confed.*, vol. 182, 2021, doi: 10.1016/j.measurement.2021.109654.
- [4] A. Bouzid, S. Chidami, T. Q. Lailier, A. C. García, T. Ould-bachir, and J. Chaouki, "Innovative non-invasive and non-intrusive precision thermometry in stainless-steel tanks using ultrasound transducers," *Sensors*, vol. 24, no. 11, p. 3404, 2024, doi: 10.3390/s24113404.
- [5] L. Zhai, Y. Huang, J. Qiao, B. Xu, and N. Jin, "Measurement of Gas Holdup in Slug Region of Horizontal Oil-Gas-Water Three-Phase Flow by a Distributed Ultrasonic Sensor," *IEEE Sens. J.*, vol. 24, no. 3, pp. 2547–2557, 2024, doi: 10.1109/JSEN.2023.3342029.
- [6] C. L. Goh, R. A. Rahim, H. F. Rahiman, T. Zhen Cong, and Y. A. Wahad, "Simulation and experimental study of the sensor emitting frequency for ultrasonic tomography system in a conducting pipe," *Flow Meas. Instrum.*, vol. 54, no. July 2015, pp. 158–171, 2017, doi: 10.1016/j.flowmeasinst.2017.01.003.
- [7] N. Hiremath, V. Kumar, N. Motahari, and D. Shukla, "An Overview of Acoustic Impedance Measurement Techniques and Future Prospects," *Metrology*, vol. 1, no. 1, pp. 17–38, 2021, doi: 10.3390/metrology1010002.
- [8] P. Regtien and E. Dertien, *Sensors for Mechatronics*. 2018.